SUPPLEMENTARY INFORMATION
for Shen et al.,
Nature Manuscript #2006-03-02695B

Supplemental figure 1

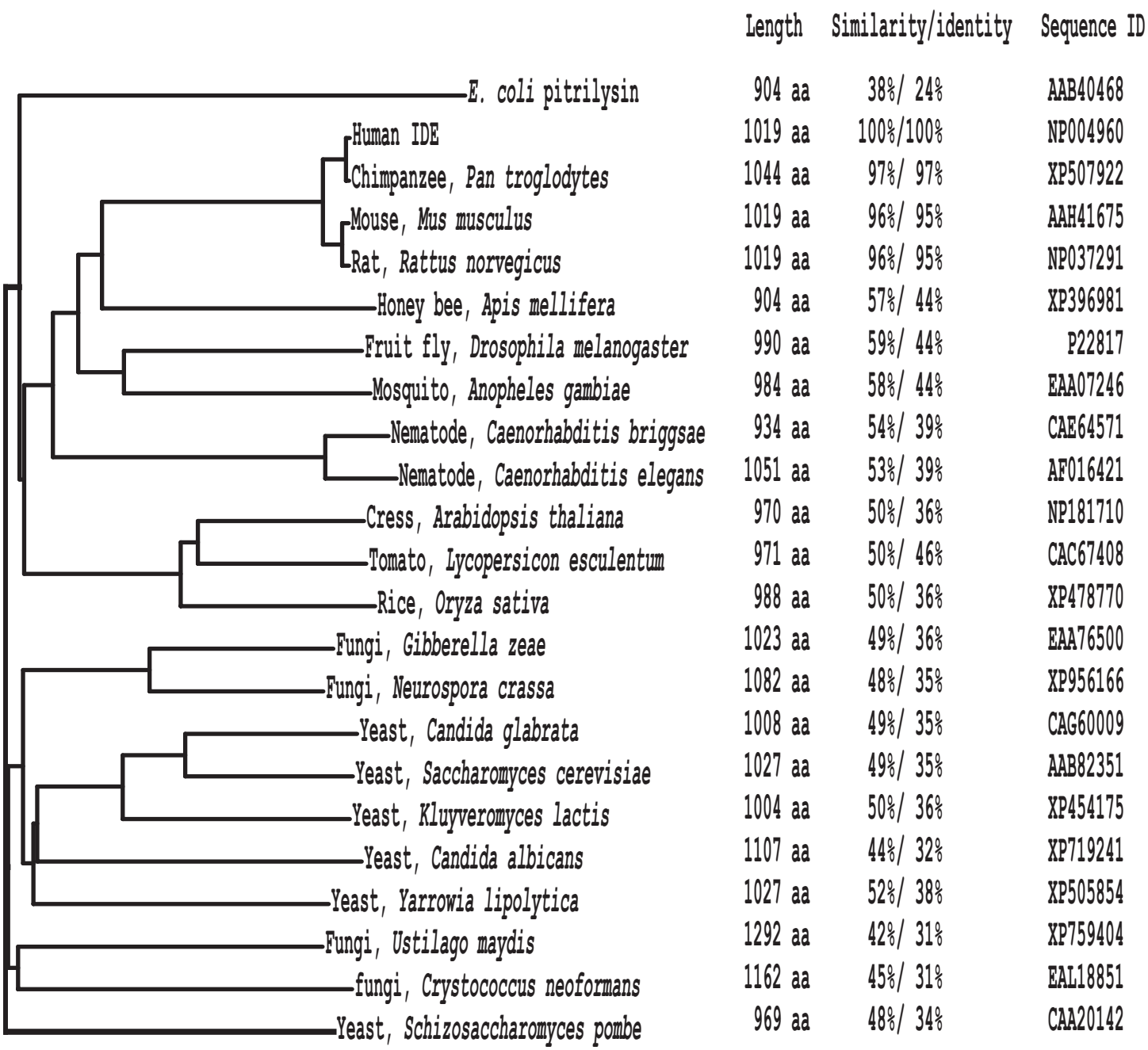

Phylogenic tree of insulin degrading enzyme. The amino acid length and protein sequence ID of IDE homologues from mammals, insects, round worms, plants, and fungi are indicated. The sequence similarity and identity of IDE is compared to human IDE.

Supplemental figure 2

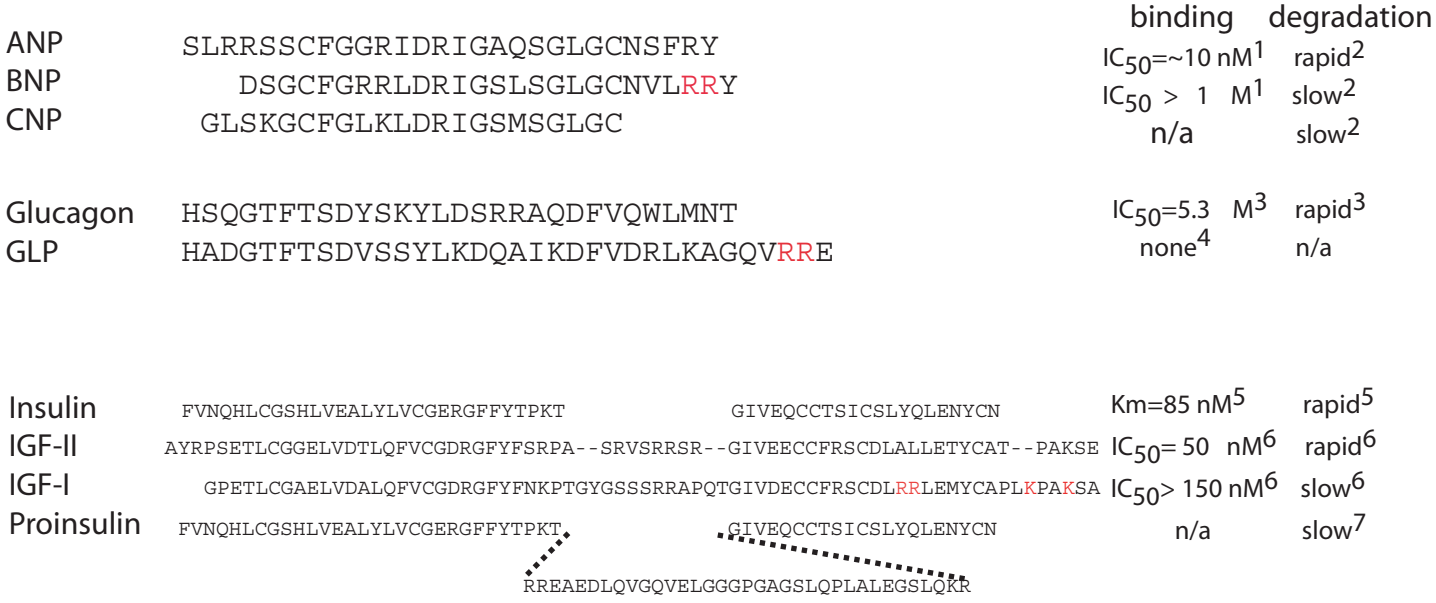

Sequence alignment of IDE interacting peptides. ANP, Atrial natriuretic peptide; BNP, Brain natriuretic peptide; CNP, C-type natriuretic peptide; GLP, glucagon-like peptide; IGF, insulin-like growth factor. Glucagon, GLP, insulin, IGF-I, IGF-II and proinsulin are from human. ANP is from rat, and BNP and CNP are from pig. The degradation of Insulin and proinsulin were measured using human IDE while ANP, BNP, CNP, glucagon, GLP, IGF-II and IGF-I were performed using rat IDE. Postively charged residues at the C-terminus of peptides that are not preferred by IDE are colored red. n/a means not available.

1 Muller, D., et al., Atrial natriuretic peptide (ANP) is a high-affinity substrate for rat insulin-degrading enzyme. Eur. J. Biochem., 202:285-292, 1991.
2 Muller, D., et al., Rat Insulin-degrading enzyme: cleavage pattern of the natriuretic peptide hormones ANP, BNP and CNP revealed by HPLC and mass spectrometry. Biochemistry, 31:11138-11143, 1992.
3 Duckworth, W. C. & Kitabchi, A. E., Insulin and glucagon degradation by the same enzyme. Diabetes, 23:536-543, 1974.
4 Authier, F., et al., Degradation of the cleaved leader peptide of thiolase by a peroxisomal proteinase. Proc. Nat. Acad. Sci. USA, 92:3859-3863, 1995.
5 Chesneau V. & Rosner, M. R., Functional human insulin-degrading enzyme can be expressed in bacteria. Protein Expr. Purif., 19:91-98, 2000.
6 Misbin, R. I., et al., Inhibition of insulin degradation by insulin-like growth factors. Endocrinology, 113:1525-1527, 1983.
7 Kitabchi, A. E., et al., Direct measurement of proinsulin in human plasma by the use of an insulin-degrading enzyme. J. Clin. Invest., 50: 1792-1799, 1971.

Supplemental figure 3

A

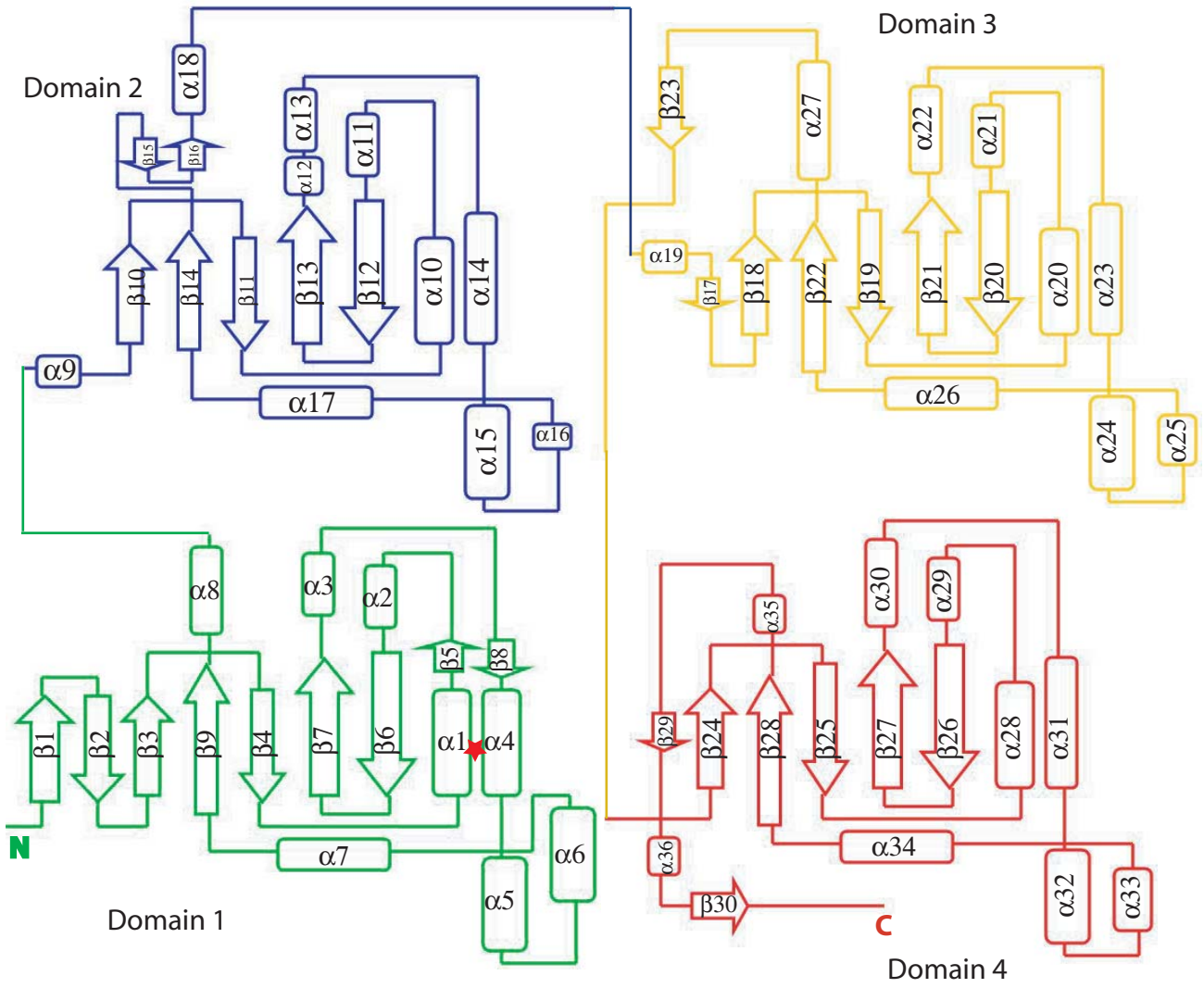

B

Similarity(%)/ Identity(%)	Domain 1	Domain 2	Domain 3
Domain 2	21/11		
Domain 3	21/12	24/12	
Domain 4	20/7	24/15	15/7

Domain analysis of human insulin-degrading enzyme (IDE). (**A**) Secondary structure representation of IDE. The four IDE domains are colored green, blue, yellow and red. The location of the zinc metal binding, catalytic site of IDE is marked by a red star. (**B**) Pairwise sequence comparison of the four IDE domains.

Supplemental figure 4A

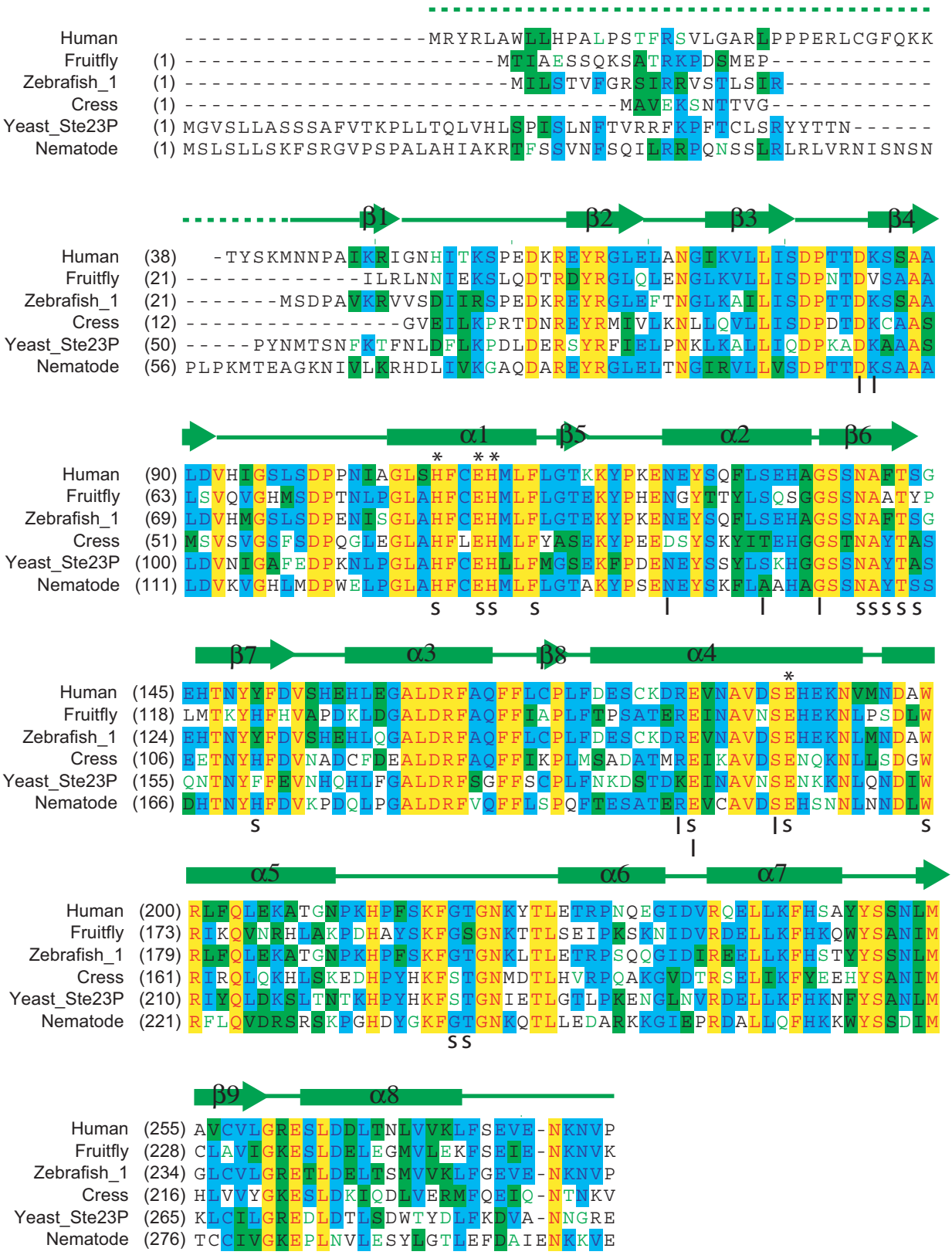

Sequence alignment of IDE domain 1 (A), domain 2 (B), domain 3 (C), and domain 4 (D). Residues below asterisks indicate the conserved residues for zinc binding and catalysis. Residues above "S" are those that are involved in substrate binding. Residues above "I" are those that are located at the interface between IDE-N and IDE-C and are involved in the interaction between these two domains (see the list in Supplemental figure 4E). Residues in red with yellow shade are residues that are identical within six members of IDE. Residues in blue are mostly identical among IDE family. Residue in green shade are homologous residues among IDE family. (E) List of atoms from IDE-N and IDE-C that are in close contact and the distance measurement.

Supplemental figure 4B

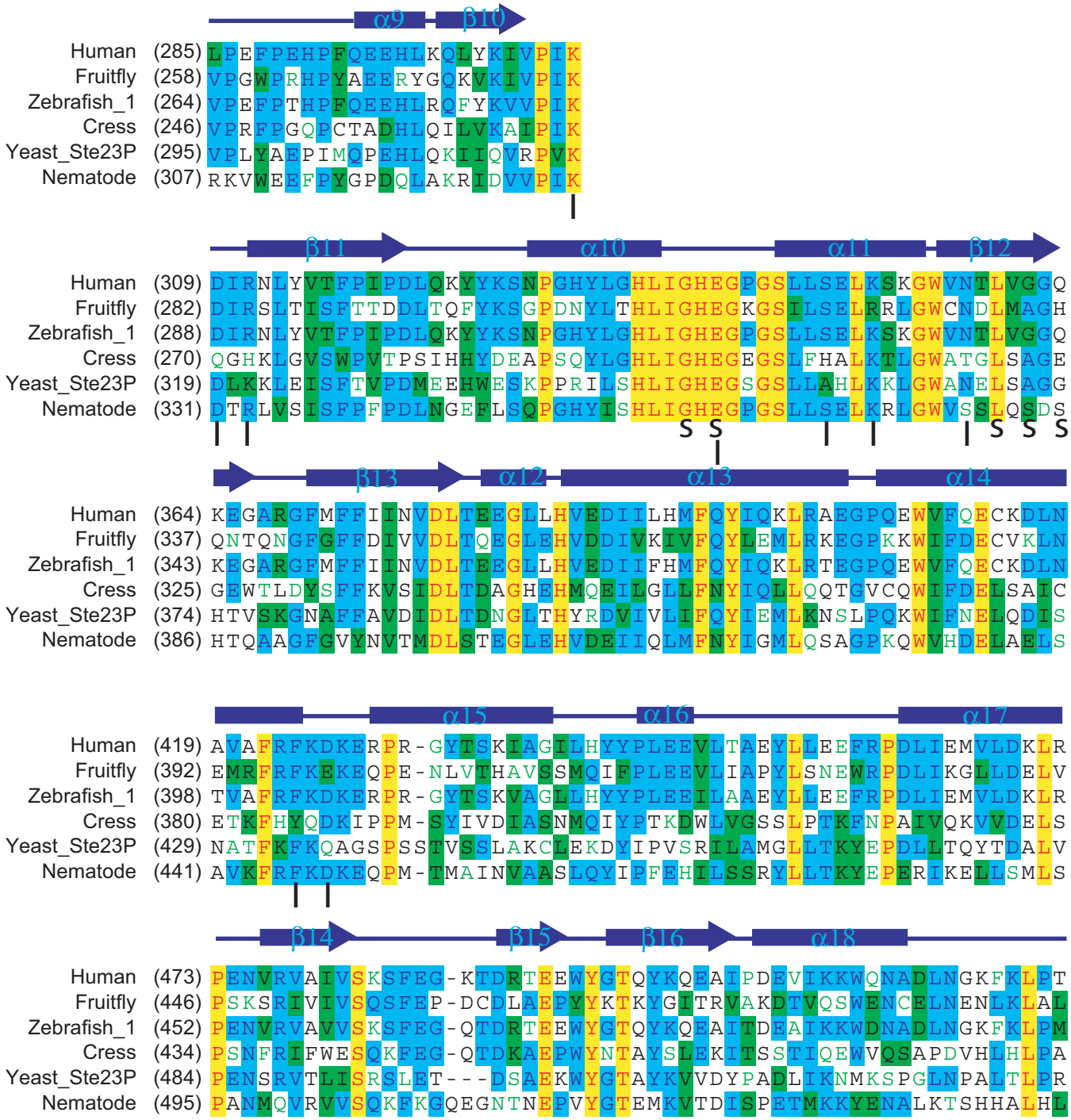

IDE domain 2 alignment. Residues above "S" are those that are involved in substrate binding. Residues above "I" are those that are located at the interface between IDE-N and IDE-C and are involved in the interaction between these two domains. Residues in red with yellow shade are residues that are identical within six members of IDE. Residues in blue are mostly identical residues and those in green shade are homologous residues.

Supplemental figure 4C

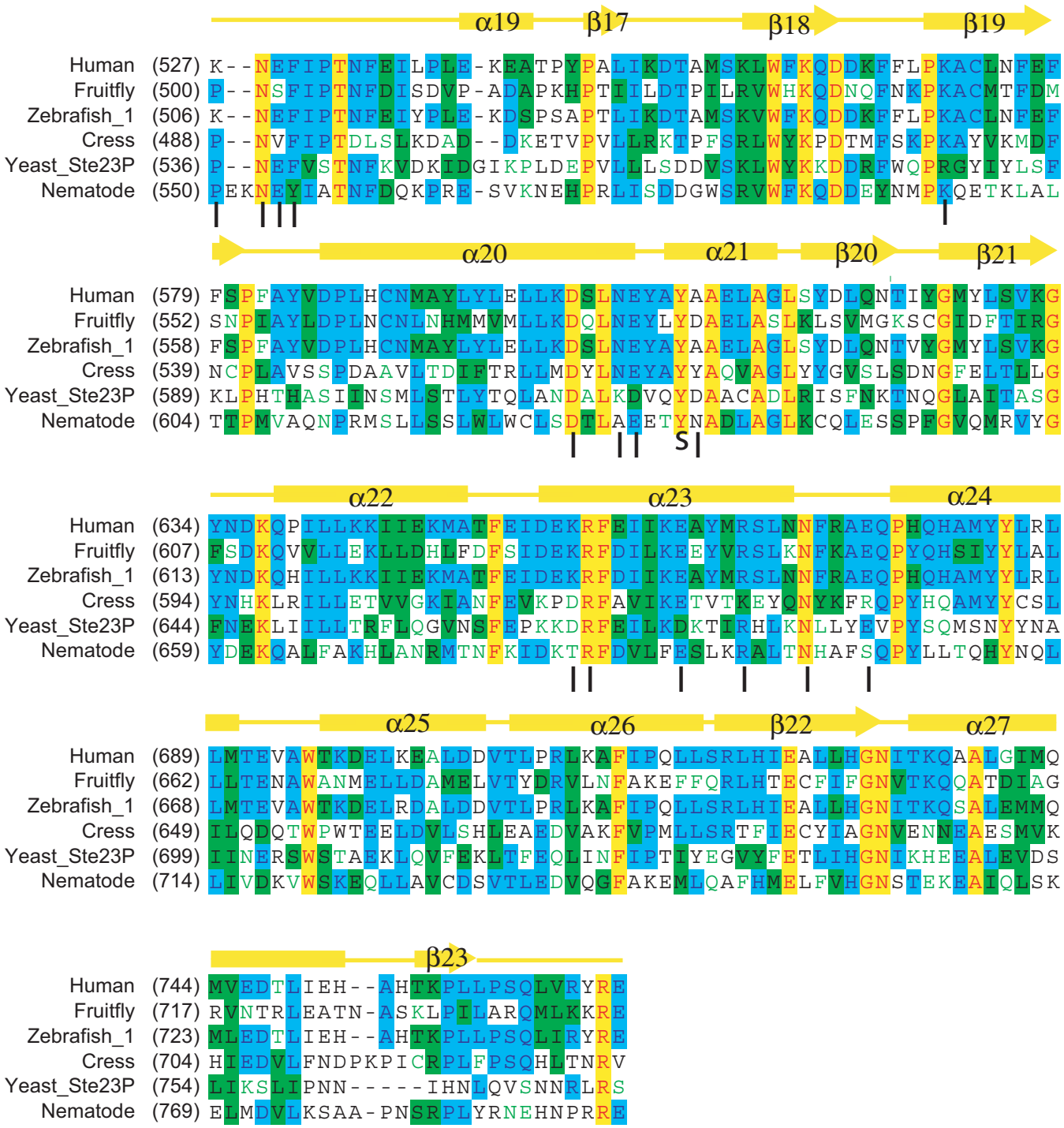

IDE domain 3 alignment. Residues above "S" are those that are involved in substrate binding. Residues above "I" are those that are located at the interface between IDE-N and IDE-C and are involved in the interaction between these two domains. Residues in red with yellow shade are residues that are identical within six members of IDE. Residues in blue are mostly identical residues and those in green shade are homologous

Supplemental figure 4D

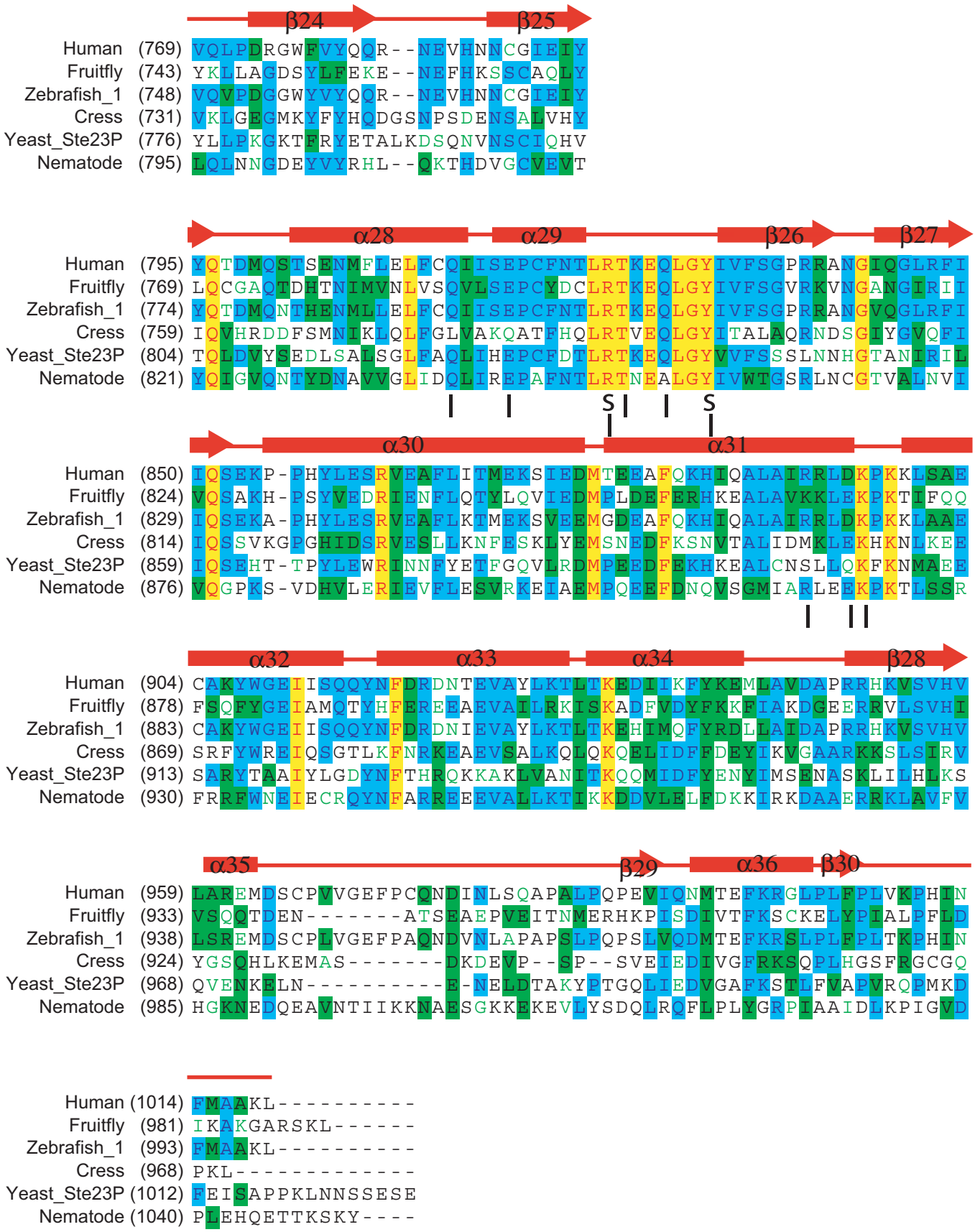

IDE domain 4 alignment. Residues above "S" are those that are involved in substrate binding. Residues above "I" are those that are located at the interface between IDE-N and IDE-C and are involved in the interaction between these two domains. Residues in red with yellow shade are residues that are identical within six members of IDE. Residues in blue are mostly identical residues and those in green shade are homologous residues.

Supplemental figure 4E

Atoms from IDE-N			Atoms from IDE-C			distance (Angstrom)
ASP	84	OD2	LYS	896	N	3.1
LYS	85	NZ	ASP	895	OD2	3.3
ASN	125	OD1	GLU	817	OE1	3.1
SER	132	O	GLN	813	NE2	3.2
SER	132	O	ARG	892	NH2	3.3
GLY	136	O	ARG	892	NH1	2.6
ARG	181	NH1	THR	825	O	2.8
GLU	182	OE1	ARG	824	NH2	3.2
GLU	182	OE2	GLN	828	OE1	3.3
ALA	185	N	GLN	828	NE2	3.1
SER	188	OG	TYR	831	N	2.7
LYS	308	NZ	GLU	676	OE1	2.8
ASP	309	O	ARG	668	NH1	2.8
ASP	309	N	ASN	672	ND2	2.8
ARG	311	NH2	GLU	664	OE2	2.5
ARG	311	NH2	ARG	668	NE	3.1
GLU	341	OE2	ASN	605	OD1	2.9
SER	348	OG	GLU	606	OE2	2.7
LYS	351	NZ	ASP	602	OD2	2.9
LYS	351	O	LYS	657	NZ	2.9
ASN	357	OD1	ARG	658	NH2	3.0
PHE	424	O	LYS	571	NZ	2.8
ASP	426	OD1	LYS	571	NZ	2.9
LYS	527	O	GLU	529	N	3.1
ASN	528	OD1	PHE	530	N	2.9
ASN	528	ND2	ALA	610	O	2.9

Supplemental figure 5

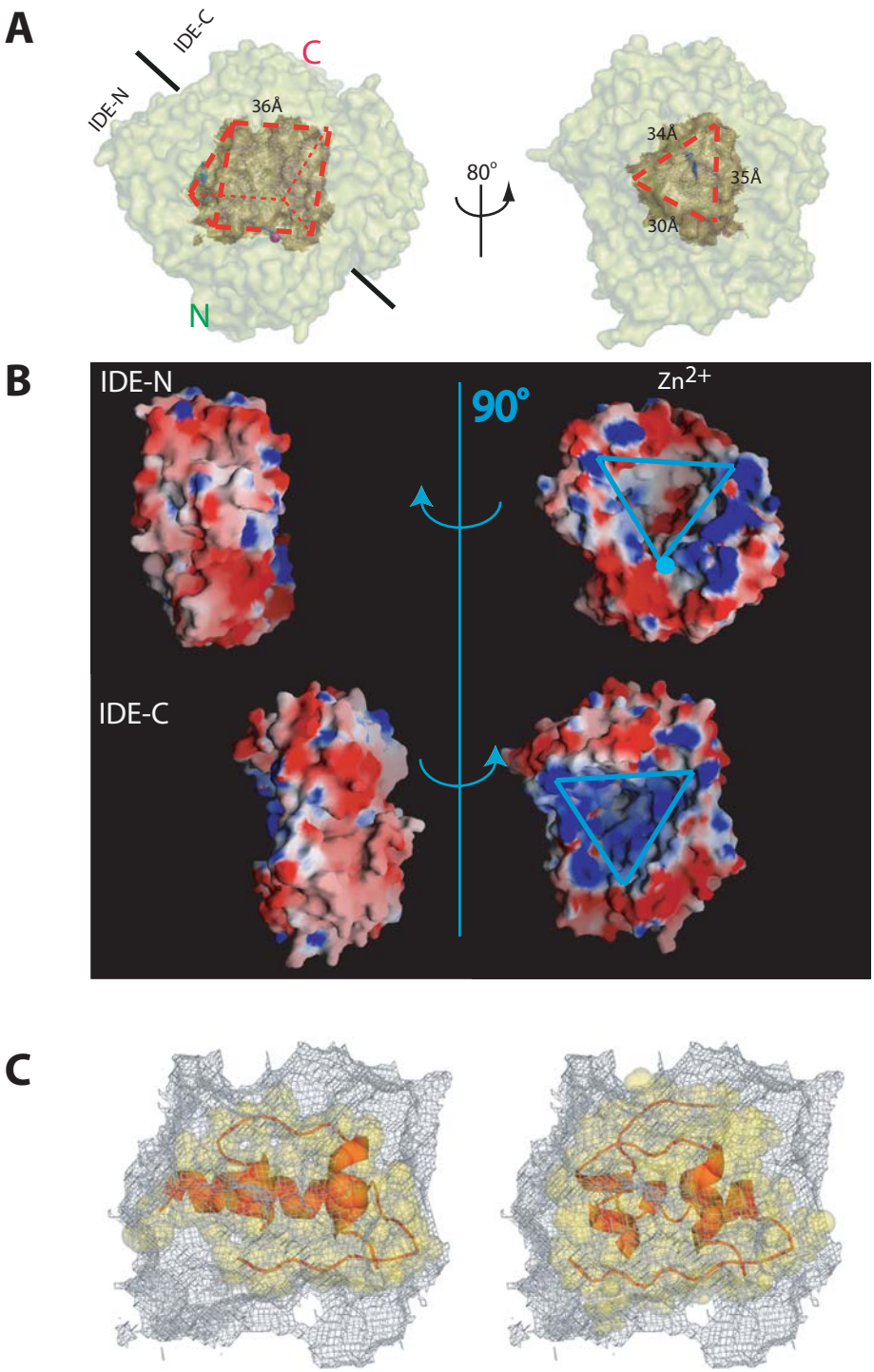

Analysis of the substrate binding chamber of IDE. (**A**) Surface representation of the IDE substrate binding chamber. Surface of IDE is shown in light yellow and the substrate binding chamber is colored brown Zinc ion and insulin are colored magenta and orange, respectively. (**B**) Electrostatic surface representation of IDE-N and IDE-C. Triangles colored cyan indicate the shape of the substrate binding chamber. The GRASP program (Nicholls et al., Proteins 11:281, 1991) was used to calculate the surface potential. Negative surface is colored red, positive surface blue, and neutral surface white. (**C**) Models to depict how the enclosed substrate binding chamber is just large enough to accommodate intact insulin at its R state (left) or T-state (right). The substrate binding cavity is represented by the gray mesh. The space-filling and ribbon models of insulin (pdb code: 1G7A) are colored yellow and red, respectively.

Supplemental figure 6

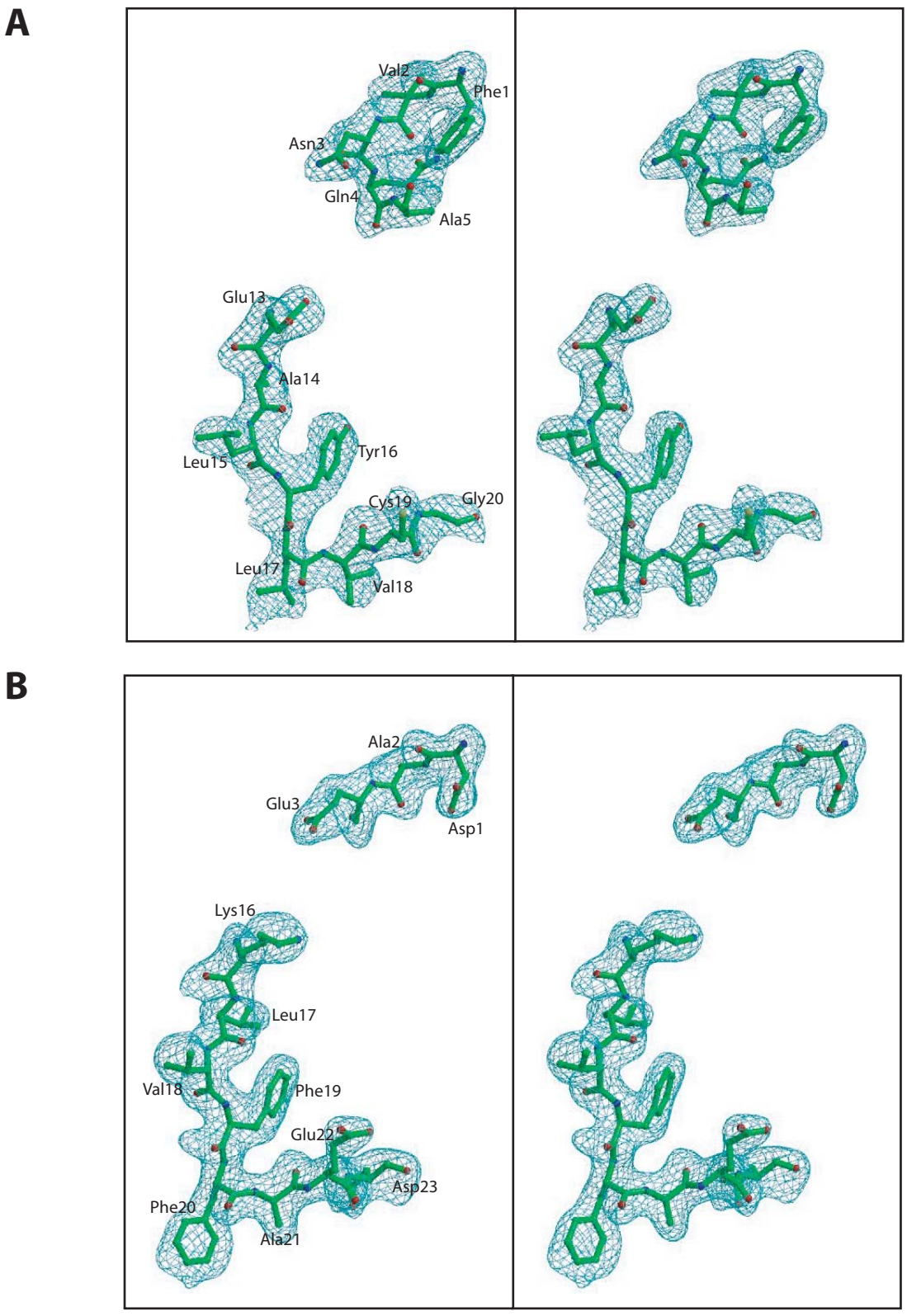

Stereo view of simulated annealing omit map contour at 3.5σ of IDE-bound insulin B chain (**A**) and IDE-bound Aβ (1-40) (**B**). The map is colored cyan and the backbone is colored green. Atoms oxygen, nitrogen and carbon are colored red, blue, and green, respectively.

Supplemental figure 6 (continued)

C

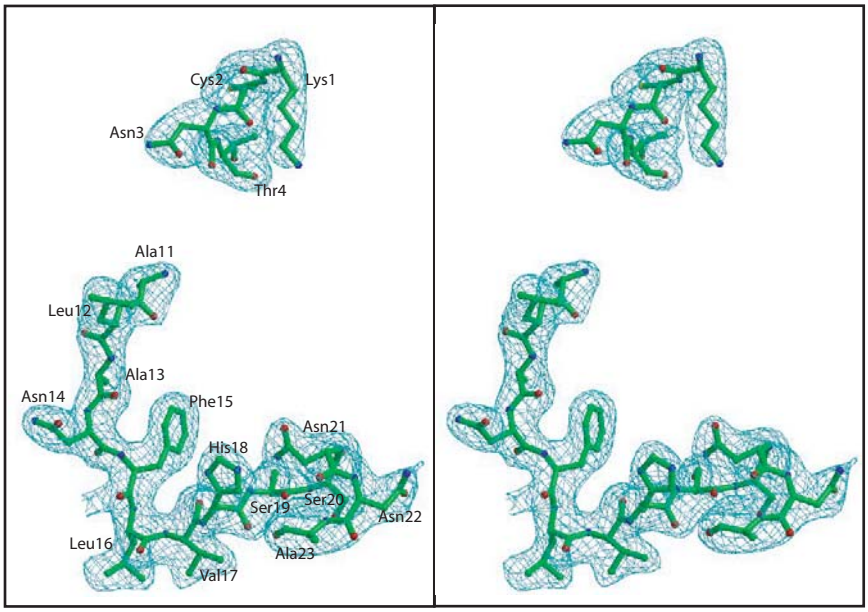

D

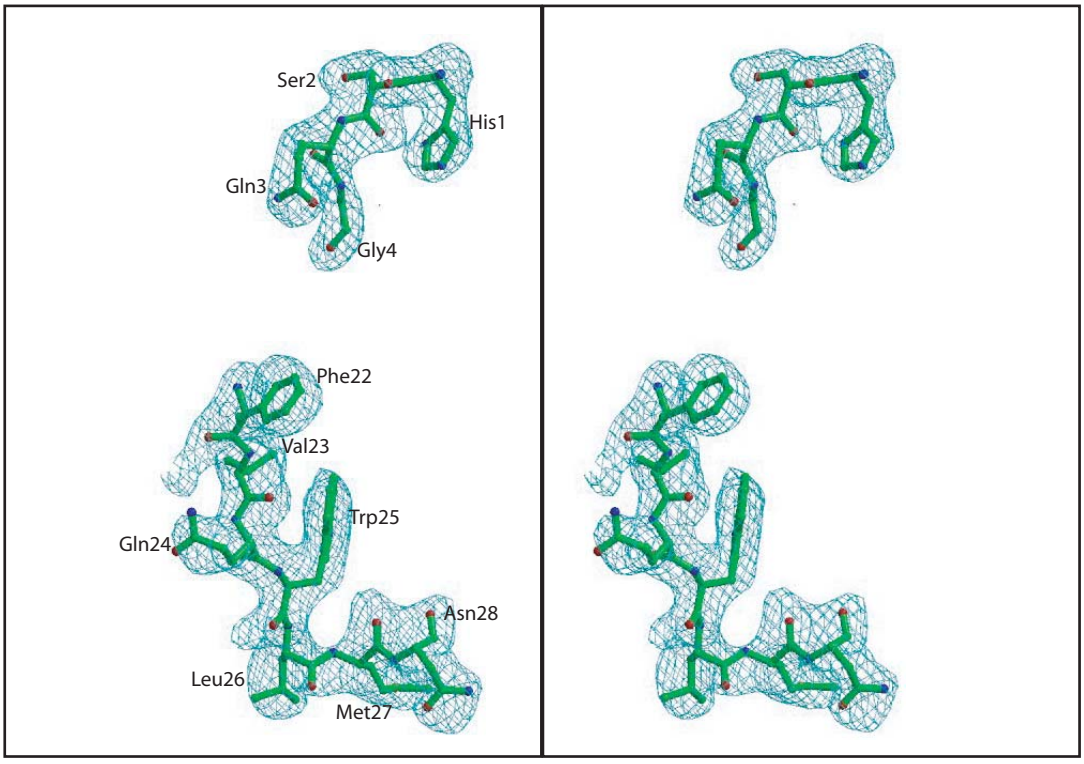

Stereo view of simulated annealing omit map contour at 3.5σ of IDE-bound amylin (**C**) and IDE-bound glucagon (**D**). The map is colored cyan and the backbone is colored green. Atoms oxygen, nitrogen and carbon are colored red, blue, and green, respectively.

Supplemental figure 6 (continued)

E

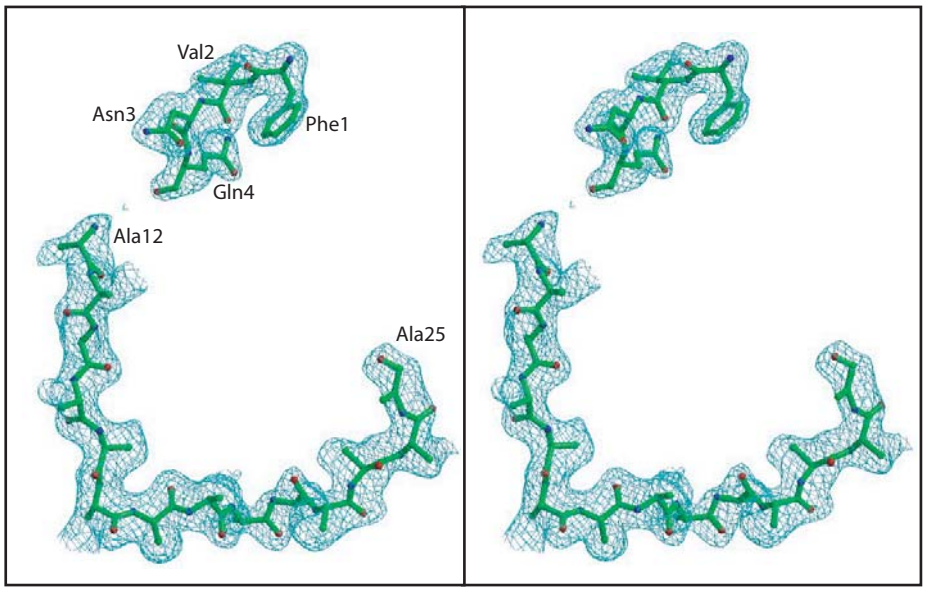

Stereo view of simulated annealing omit map contour at 3.5σ of IDE-bound insulin in the presence of 5 mM EDTA (**E**). The map is colored cyan and the backbone is colored green. Atoms oxygen, nitrogen and carbon are colored red, blue, and green, respectively.

Supplemental figure 7

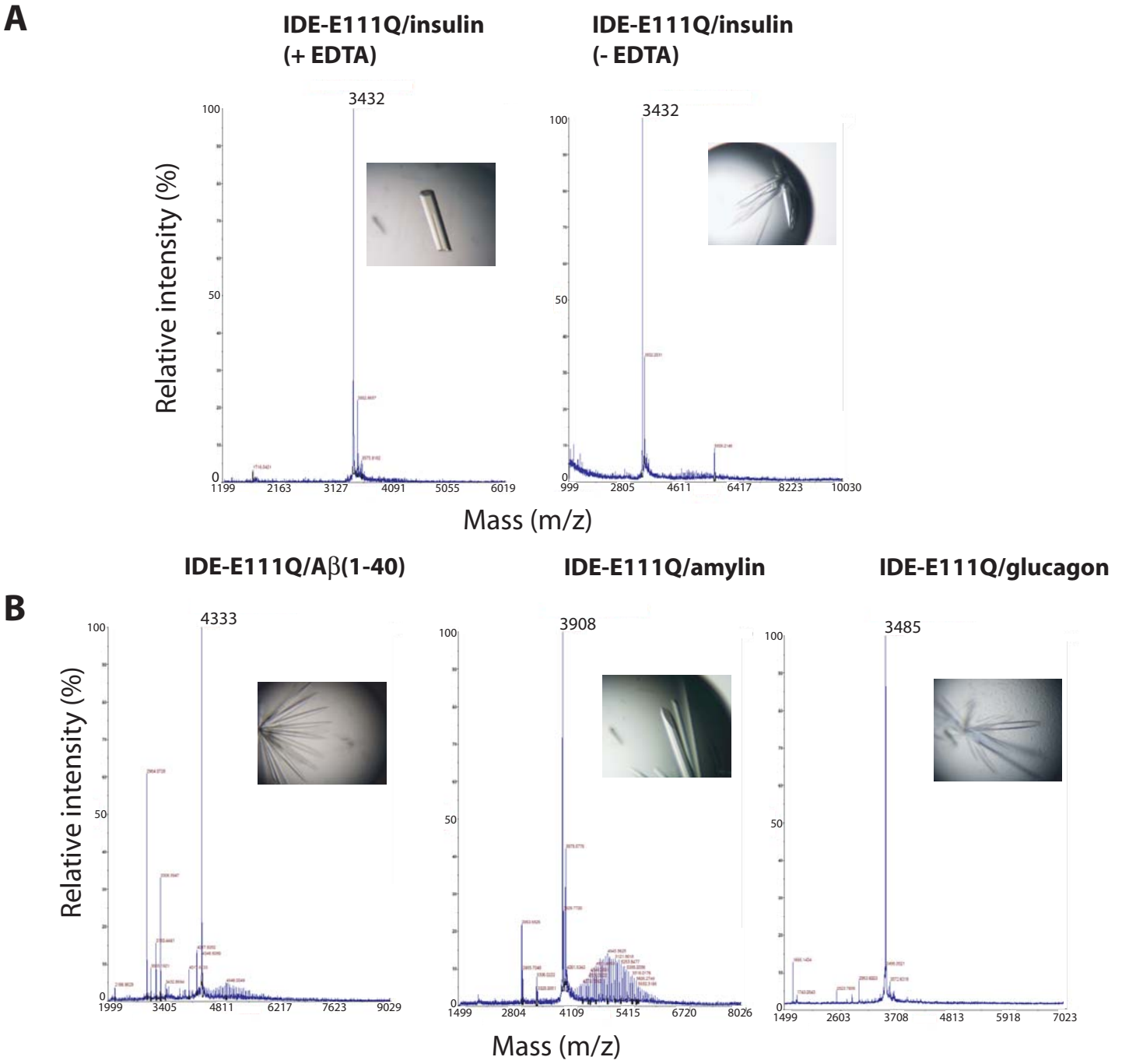

MALDI-TOF mass spectrometry analysis of crystals of IDE-substrate complexes. Mass-spec analysis of peptides eluted from IDE-insulin B chain crystals in the presence and absence of EDTA (**A**) and those from crystals of IDE in complex with Aβ1-40, amylin, and glucagon in the presence of EDTA (**B**). The expected molecular weight of these IDE substrates are as following: insulin B chain, 3431 dalton (Da); Aβ 1-40, 4331 Da, amylin, 3907 Da; and glucagon, 3484 Da. EDTA is used to chelate zinc ion to further reduce the catalysis of the IDE-E111Q mutant. All of the crystals are grown in the presence of 5 mM Tris(2-carboxyethyl) phosphine (TCEP, reducing agent). The disulfide bond of insulin is presumably reduced in the crystal of IDE-E111Q in complex with insulin. For MALDI-ToF experiments, 5 µl of samples were mixed with equal volume of 0.1% trifluoroacetic acid (TFA) and passed through a C-18 ZipTip (Millipore). 1 µl treated samples were then mixed with matrix (α-cyano-4-hydroxycinn) and spotted on the metal plate (ABI). The experiment was done using ABI 4700 Maldi TOF/TOF MS.

Supplemental figure 8

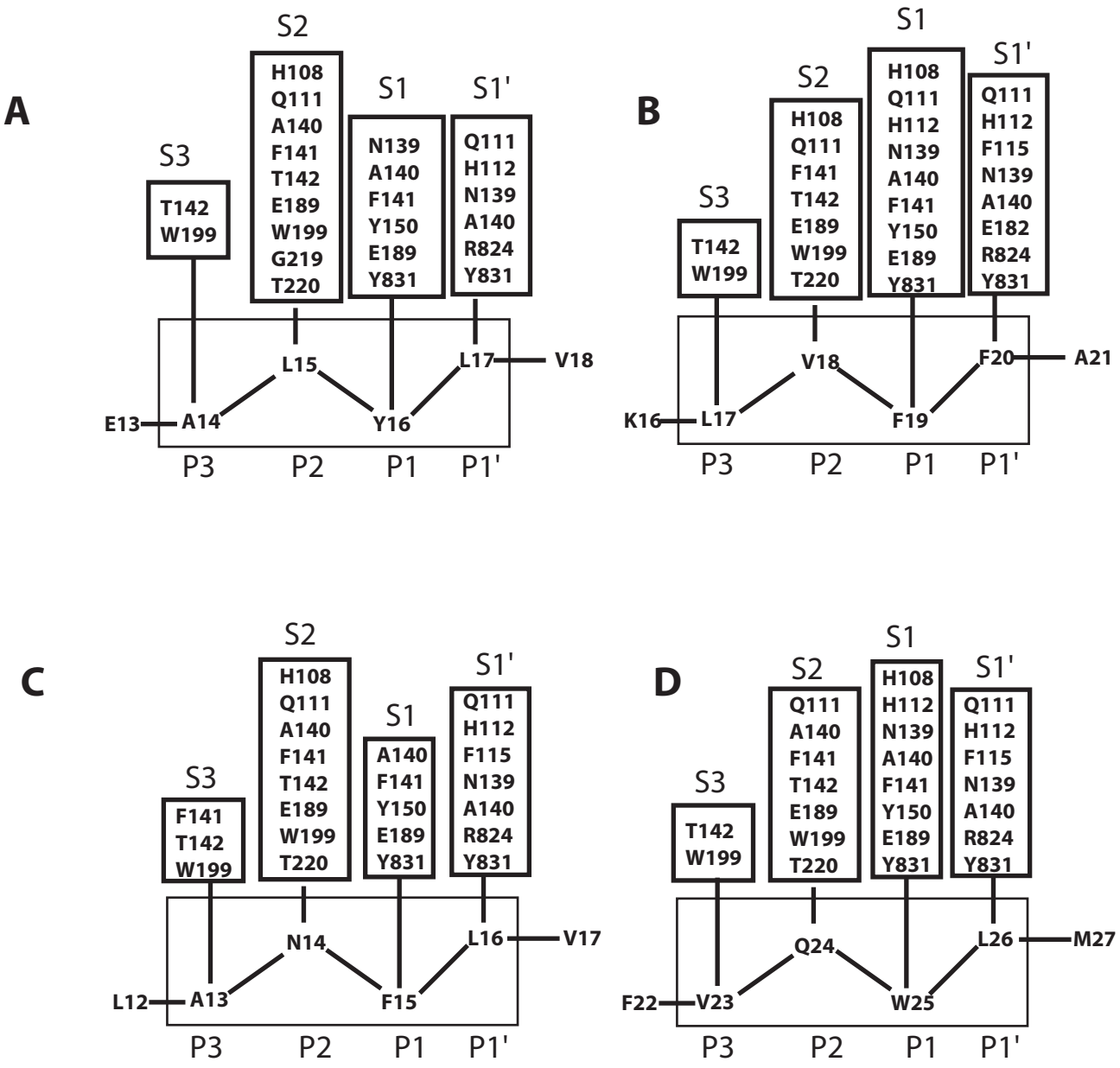

Detailed interactions of residues at the IDE catalytic cleft with the cleavage sites of insulin B chain (**A**), Aβ1-40 (**B**), amylin (**C**), and glucagon (**D**).
The cut-off distance is 4.0Å.

Supplemental figure 9

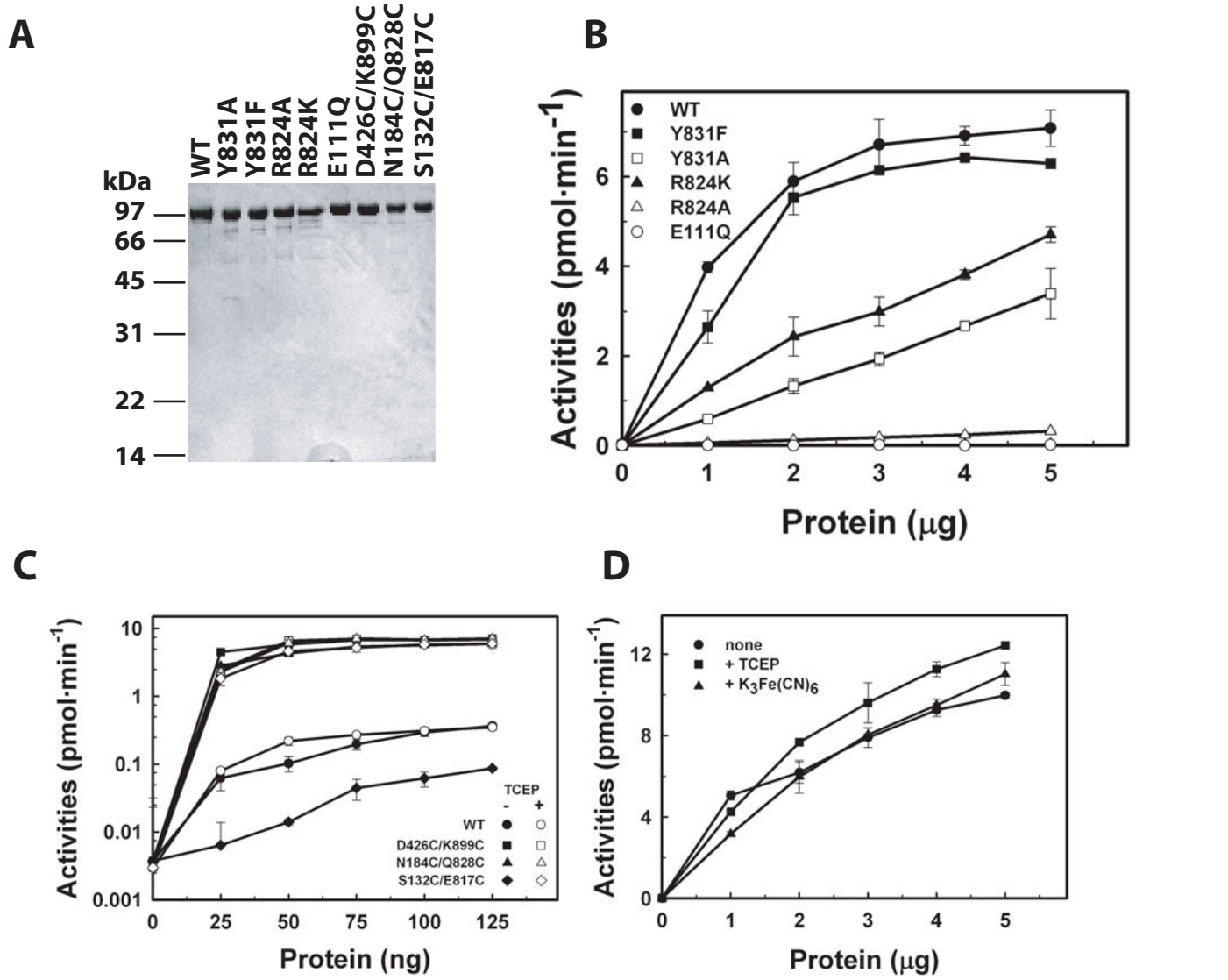

Enzymatic activities of IDE mutants.

(A) Coomassie blue staining of purified IDE proteins. 1.5 g protein was loaded on 13% SDS-PAGE gel.
(B) Activities of IDE mutants which had a single mutation in domain 4 or the catalytic base in domain 1. The indicated quantities of IDE proteins were used and the fluorescence intensity was measured after the reaction was performed for one hour.
(C) Activities of IDE double cysteine mutants in the absence (filled symbols) and presence (open symbols) of TCEP. The assays were done after one hour incubation using indicated quantities of IDE.
(D) Comparison of IDE wild type activities in the presence and absence of 1mM reducing agent, TCEP or 1 mM oxidizing agent, $K_3Fe(CN)_6$. The reaction was performed for 30 minutes under identical conditions as described in figure 3D and 3E.

Supplemental figure 10

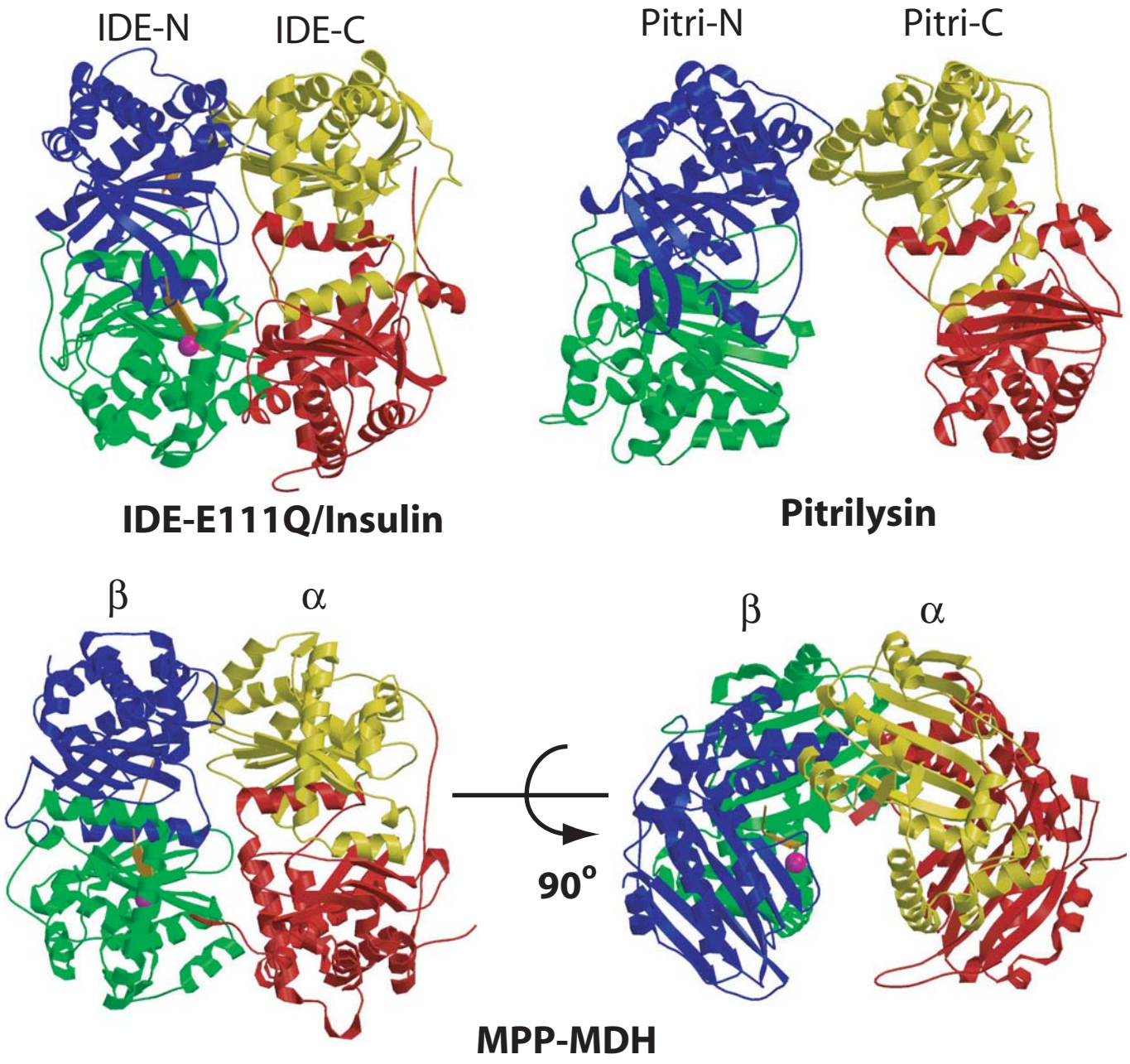

Structural comparison of insulin B chain-bound IDE with substrate-free *E. coli* pitrilysin (pdb code: 1Q2L) and Yeast mitochondria processing peptidase (MPP, pdb code:1HR9). Four structurally homologous domains are colored green, blue, yellow, and red, respectively. Insulin and Zn ion are colored orange and magenta. Domains of MPP β and α subunit are colored based on the corresponding domains of IDE. Peptide substrate from the N-terminal signal peptide of Malate dehydrogenase (MDH) and zinc ion are colored orange and magenta, respectively. It is worth noting that the opening of MPP is completely different from pitrilysin.

Supplemental figure 11

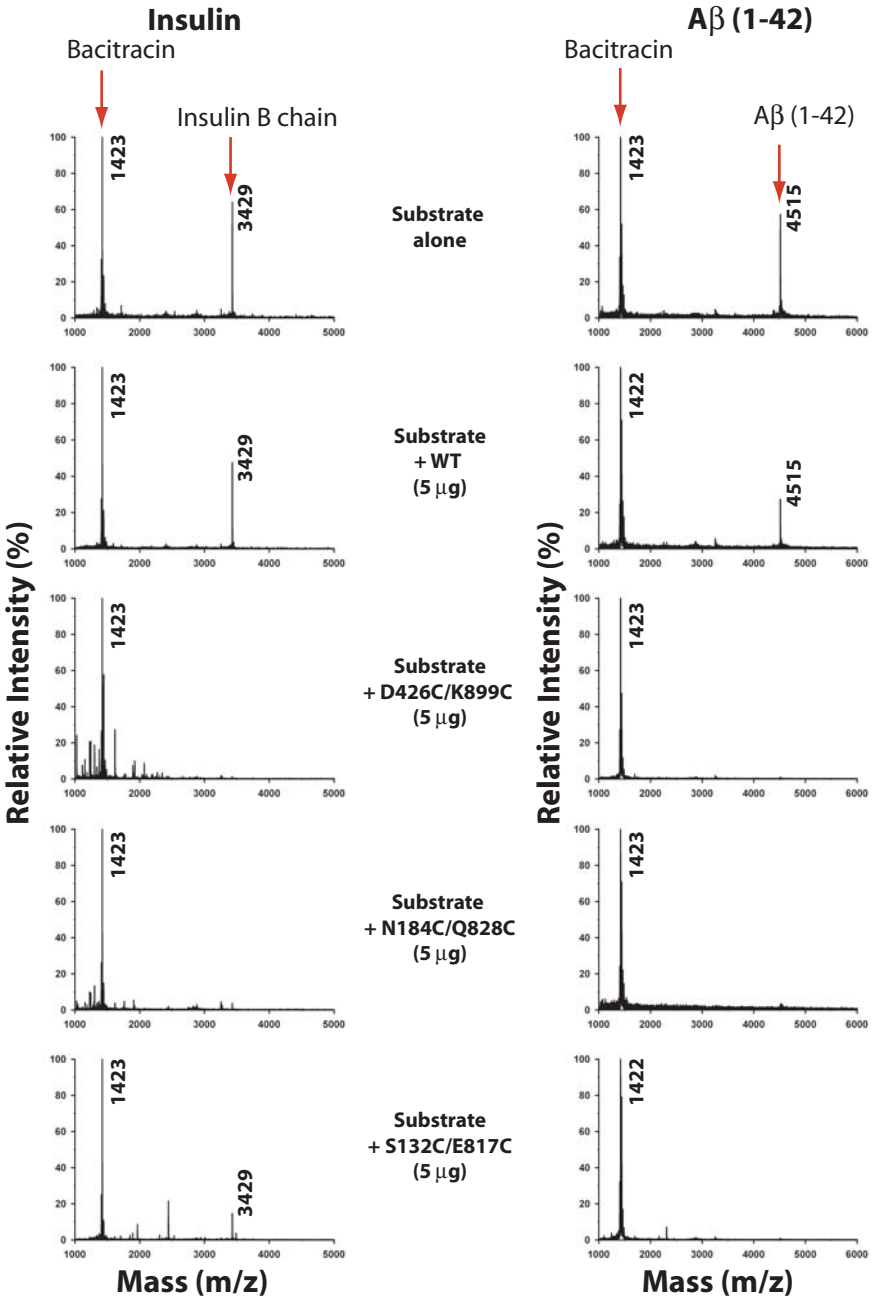

MALDI-ToF mass spectrometry analysis of the degradation of insulin and Aβ (1-42) by IDE mutants. To perform the reactions, 10 µl buffer (20 mM HEPES, pH7.2, 1mM TCEP) was incubated with 5 µg IDE protein (5µl of 1 mg/ml protein solution) at room temperature for 5 minutes. The reaction was started by adding 5 µg insulin or 15 µg Aβ (1-42) into the above mixture and then incubated for one hour at 37 °C. The reaction was stopped by the addition of 5 µl TFA(10%) . The 5 µg bacitracin was then added to serve as a recovery standard of mass spectrometry. The reaction solution (0.5 µl) was mixed with 0.5 µl matrix (α-cyano-4-hydroxycinn) and directly spotted on the metal plate as described in supplemental figure 7. The estimated molecular weight of bacitracin, insulin B chain and Aβ (1-42) are 1,423 daltons, 3,431 daltons and 4,514 daltons, respectively. Date presented are representative of two independent experiments. This experiment demonstrates that, under identical reaction condition all three double cysteine IDE mutants could degrade both insulin and Aβ(1-42) more effectively than wild type IDE. This suggests that all three IDE mutants under reduced condition (+ TCEP) are substantially more active than wild type IDE. This result is consistent with our finding using fluorogenic substrate V.

Supplemental figure 12

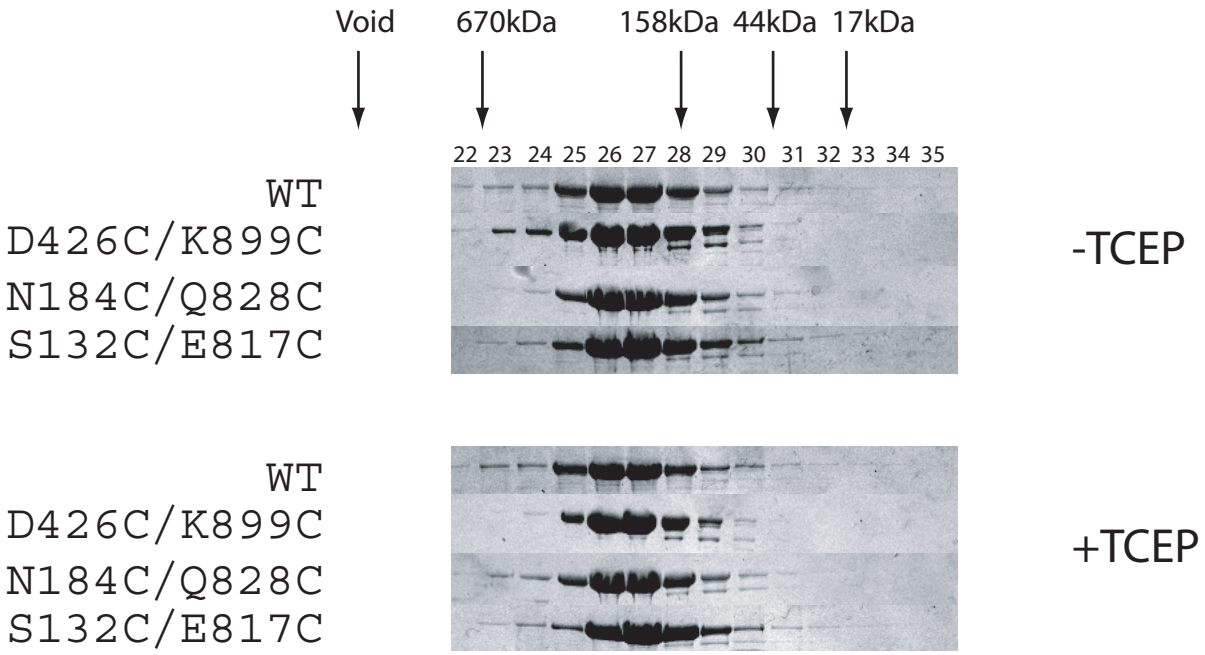

Oligomeric state of wild type IDE and its mutants. Each protein (5 mg) was mixed with 0.6 ml buffer (20 mM Tris pH 8.0, 100 mM NaCl with/without 1 mM TCEP) on ice for 30 minutes and then loaded onto the superose 6 size-exclusion column (GE healthcare). The elusion was run by AKTA FPLC (GE healthcare) with a flow rate of 0.3 ml/min and fractions were collected every two minutes. The peak fractions are then run on 13% SDS-PAGE gel and the gel was stained by Coomassie staining. The gel-filtration standard (Biorad) was run under identical conditions. The molecular weight standard and fraction number are indicated above. Compared with wild type IDE, we did not observe an obvious change in the elusion profile of all three double cysteine IDE mutants. This indicates that no clear change occurs upon oligomerization of these three IDE mutants. Thus, the change of oligomerization state is unlikely to be the cause of the elevated proteolytic activity of these three IDE mutants.

Supplemental figure 13

A

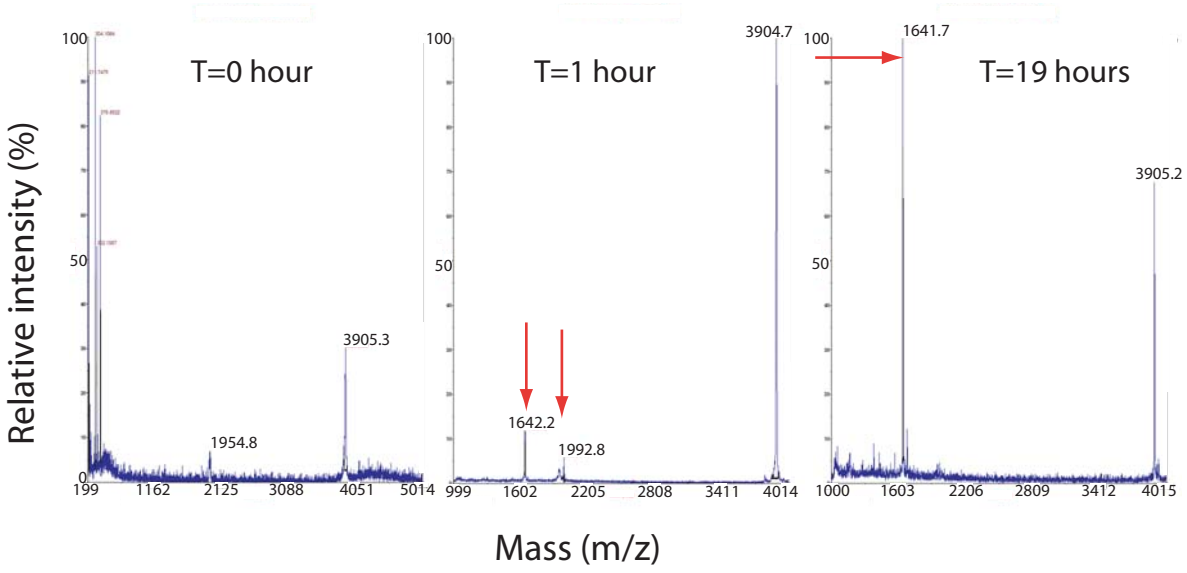

User mass	DB mass	mass difference	peptide	position
1641.700	1641.784	0.084	KCNTATCATQRLANF(L)	1-15
1642.200	1641.784	-0.416	KCNTATCATQRLANF(L)	1-15
1992.800	1992.977	0.177	(L)ANFLVHSSNNFGAILSSTN(V)	13-31

B

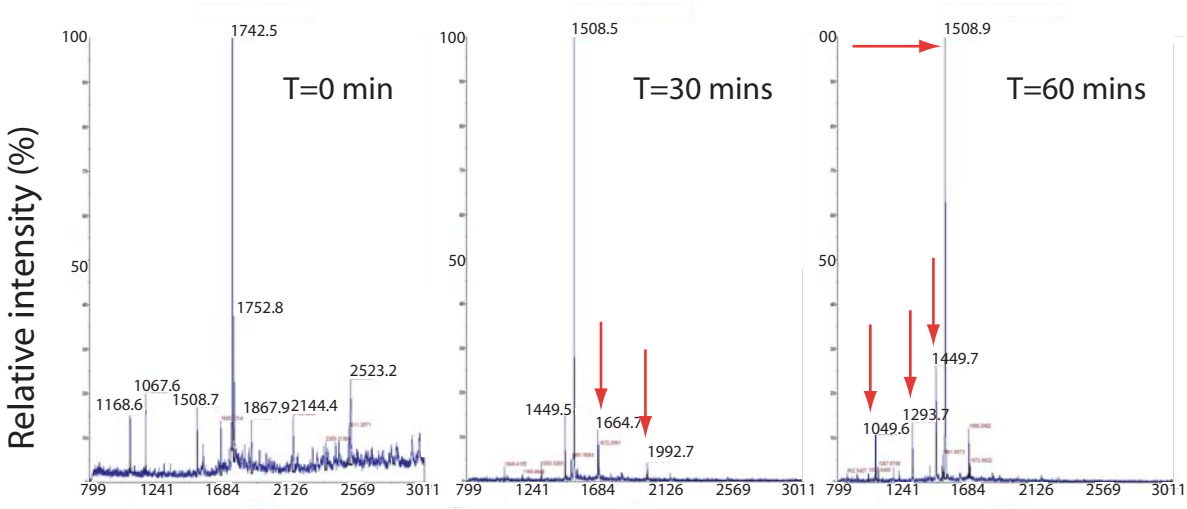

User mass	DB mass	mass difference	peptide	position
1049.600	1049.516	-0.084	(R)RAQDFVQW(L)	18-25
1293.700	1293.641	-0.059	(R)RAQDFVQWLM(N)	18-27
1449.700	1449.742	0.042	(S)RRAQDFVQWLM(N)	17-27
1508.900	1508.731	-0.169	(R)RAQDFVQWLMNT	18-29
1664.700	1664.833	0.133	(S)RRAQDFVQWLMNT	17-29
1992.700	1991.909	-0.791	HSQGTFTSDYSKYLDSR(R)	1-17

Identification of major cleavage sites of Amylin (**A**) and Glucagon (**B**). The degradation experiment was performed in the presence of 100 mM HEPES (pH 7.2), 2 mM $MnCl_2$, 2.5 M IDE and 82 M amylin or 92 M glucagon at 37°C. The reaction was stopped by mixing 10 l reaction mixture with 10 l 500 mM EDTA and 20 l 0.1% TFA. The solution was then subjected to MALDI-TOF analysis as described in supplemental figure 6. The peaks indicated by red arrows were analyzed. The cleavage sites of glucagon by IDE is consistent with partially mapped sites (Baskin, F. K., et al., Sites of cleavage of glucagon by insulin-glucagon protease, Biochem. Biophys. Res. Commun., 67:163-169, 1975; Rose, K., et al., Insulin proteinase liberates from glucagon a fragment known to have enhanced activity against Ca^{2+} + Mg^{2+} -dependent ATPase, Biochem. J., 256:847-851, 1988.)

Supplemental figure 14

A

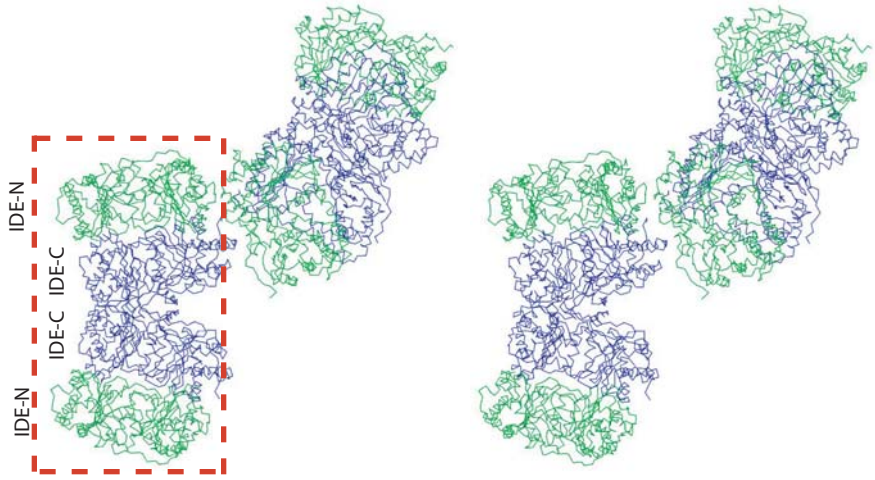

B

Atoms from 1st IDE molecule			Atoms from 2nd IDE molecule			Distance (Angstrom)
Glu	692A OE2	...	Glu	692B OE2	...	2.90
Asp	706A OD2	...	Arg	722B NH1	...	2.51
Asp	706A OD2	...	Arg	722B NH2	...	2.63
Arg	711A NE	...	Gln	718B OE1	...	3.14
Arg	722A NH1	...	Asp	706B OD2	...	3.00
Lys	756A NZ	...	Asp	706B OD2	...	2.86
Arg	767A NH1	...	Leu	1002B O	...	2.79
Arg	767A NH2	...	Lys	999B O	...	2.83
Lys	999A O	...	Arg	767B NH2	...	3.02
Arg	1000A NH2	...	Val	1008B O	...	3.10
Arg	1000A O	...	Leu	1007B N	...	2.83
Leu	1002A O	...	Arg	767B NH1	...	2.84
Leu	1004A N	...	Leu	1004B O	...	2.94
Leu	1004A O	...	Leu	1004B N	...	2.92
Leu	1007A N	...	Arg	1000B O	...	2.82

C

Atoms from 1st IDE dimer			Atoms from 2nd IDE dimer			Distance (Angstrom)
Tyr	121B OH	...	Trp	409C N	...	3.29
Lys	123B NZ	...	Asp	416C OD1	...	3.07
Arg	164B NH1	...	Glu	408C OE1	...	3.03
Arg	164B NH2	...	Gln	412C NE2	...	3.18
Thr	878B OG1	...	Glu	457C OE1	...	2.53
Glu	880B OE1	...	Glu	458C OE1	...	2.79
Glu	880B OE2	...	Lys	327C NZ	...	2.67
Lys	933B NZ	...	Thr	55C OG1	...	3.20

Oligomerization of IDE molecules. (**A**) Stereo view of the IDE dimer and the crystal packing of IDE dimers. IDE-N and IDE-C are colored green and blue, respectively. Two IDE-E111Q molecules form a dimer through the interaction of IDE-C (dashed red box) in one asymmetric unit. (**B**) List of close contacts between two IDE molecules in an IDE dimer, which are largely mediated through domain 3 and the C-terminus of IDE. (**C**) List of close contacts between two IDE dimers depicted by crystal packing of an IDE dimer. This interaction could lock IDE in the closed conformation, which would prevent substrate entry and product release. This could explain why an IDE tetramer is less active than an IDE monomer or dimer (Song et al J. Biol. Chem 278:49789, 2003).

Supplemental figure 15

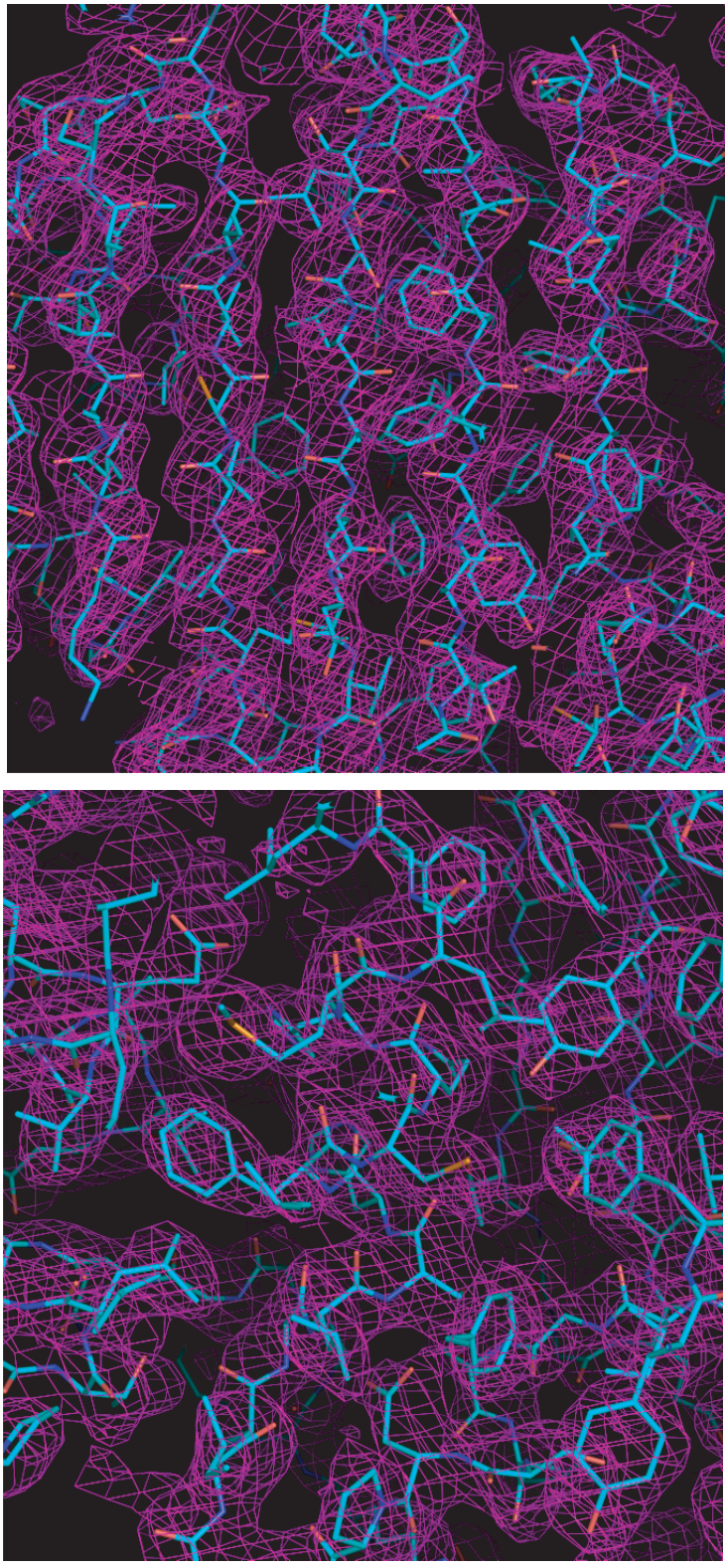

The electron density map representing β-sheet (**top**) and α-helix (**bottom**) regions of IDE from SAD phases is contoured at 1.0 σ level. The backbone is colored cyan and atoms oxygen, nitrogen, carbon and sulfur are colored red, blue, cyan, and orange, respectively.

Supplemental figure 16

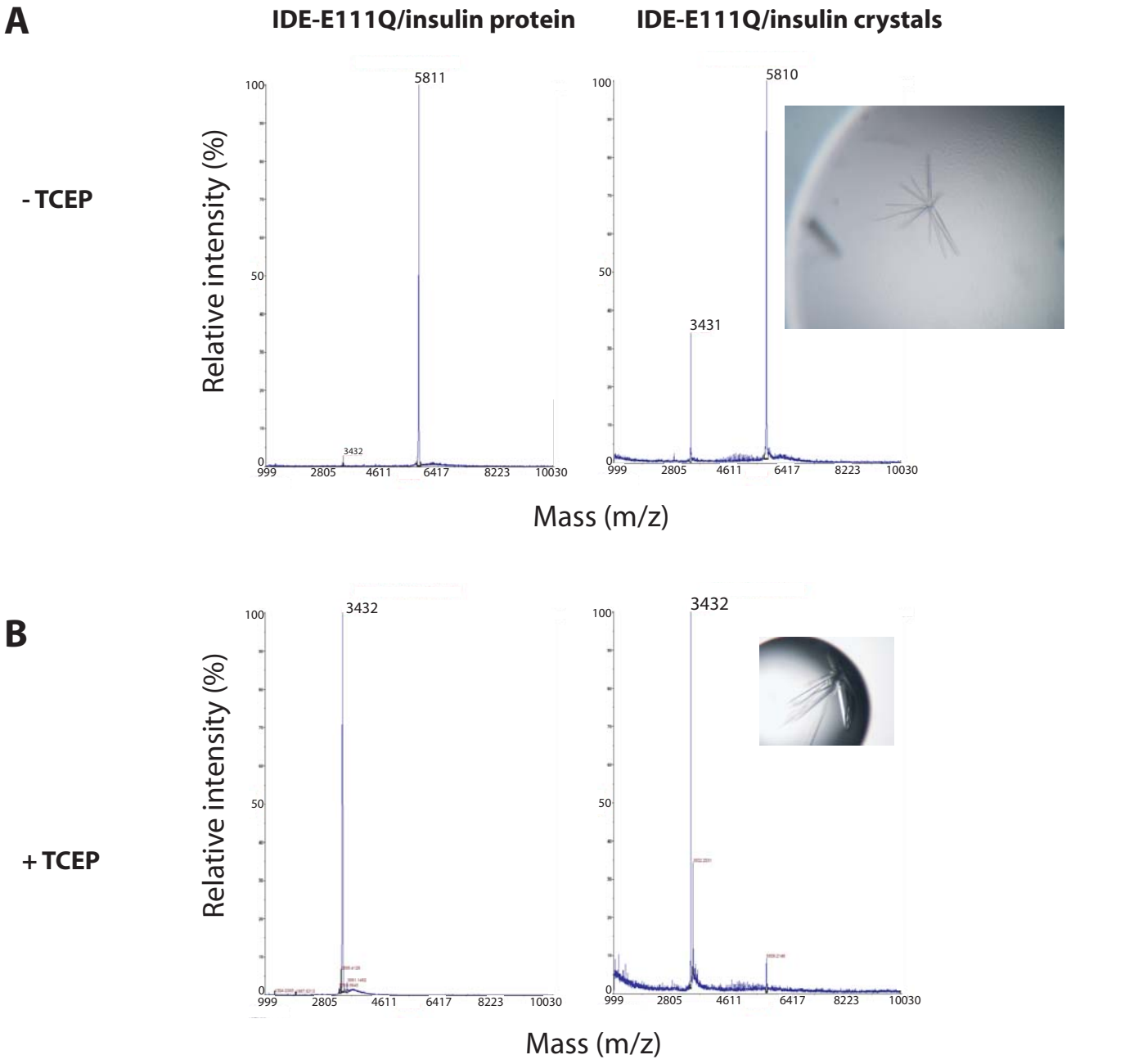

The comparison of MALDI-TOF mass spectrometry of insulin-bound IDE-E111Q complex in the absence (**A**) and presence (**B**) of TCEP. The expected molecular weight of intact insulin and insulin B chain is 5812 Da and 3431 Da, respectively. IDE-E111Q/insulin protein complex was isolated using S-200 gel-filtration chromatography (left). To know the state of insulin in the IDE-E111Q/insulin crystals, IDE-E111Q/insulin crystals were washed and dissolved by buffer (20 mM Tris, 50 mM NaCl). Crystals grown without TCEP diffract poorly. The mass spec experiment was done by the same procedure as described in supplemental figure 7.

Supplemental Table 1 Data collection and phasing statistics

Crystal name	Se-IDE-Insulin B chain-Zn^{2+}
Beamline	APS, 19-ID
Space group	$P6_5$
Wavelength (Å)	0.9793445
Unit cell (Å) *a* *c*	 263.37 90.53
Resolution (Å)	30-2.6
Unique reflections	110,675 (10,963)
Completeness (%)	100(100)
Redundancy	22.5(20.2)
Rsym(%)	9.9(64.2)
I/σ	36.6(5.4)
Se sites	34 out of 52
Figure of merit	0.506
Figure of merit after density modification	0.801

Supplemental Table 2 Data collection and refinement statistics

Data collection					
Crystal name	IDE-Insulin B-Zn^{2+}	IDE-Insulin B	IDE-Aβ (1-40)	IDE-Amylin	IDE-Glucagon
Beamline	APS, 14-BM-C	APS, 19-ID	APS, 19-ID	APS, 19-ID	APS, 19-ID
Space group	*P6₅*	*P6₅*	*P6₅*	*P6₅*	*P6₅*
Unit cell (Å)					
a	262.53	262.25	262.43	262.28	262.72
c	90.50	90.61	90.71	91.11	90.79
Resolution (Å)	50-2.25	30-2.2	30-2.1	30-2.6	30-2.5
Unique reflections	166,009 (13,956)[c]	175,528 (15,806)[c]	194,459 (15,723)[c]	108,791 (10,738)[c]	123,701 (11,802)[c]
Completeness (%)	98.0 (82.9)[c]	97.2 (87.9)[c]	94.3 (76.9)[c]	99.2 (98.9)[c]	99.6 (95.6)[c]
Redundancy[a]	10.5 (7.1)[c]	8.4 (5.7)[c]	7.6 (4.4)[c]	5.6 (5.2)[c]	10.6 (7.5)[c]
$\boldsymbol{R}_{sym}$(%)[b]	8.6 (63.8)[c]	6.4 (34.7)[c]	7.6 (55.0)[c]	10.4 (36.6)[c]	10.1 (49.5)[c]
$\boldsymbol{I} / \boldsymbol{\sigma}$	27.3 (2.6)[c]	26.5(4.6)[c]	24.2 (2.3)[c]	19.0 (5.2)[c]	23.6 (3.2)[c]
Refinement					
$\boldsymbol{R}_{cryst}$ (%)[d]	20.6	20.5	20.3	19.6	19.8
$\boldsymbol{R}_{free}$ (%)[e]	23.3	22.5	22.3	22.5	22.5
$Rmsd_{bond}$(Å)	0.007	0.009	0.008	0.007	0.007
$Rmsd_{angle}$(°)	1.3	1.3	1.3	1.3	1.3
Number of					
protein atoms	15,948	15,914	15,884	16,001	15,931
ligand atoms	12	12	12	12	12
solvent molecules	787	1044	1066	696	695
metal atoms	2	0	0	0	0
Ramachandran plot (%)					
Favorable region	90.3	90.7	91.3	90.1	89.7
Allowed region	9.7	9.3	8.6	9.8	10.2
Generously allowed region	0	0	0.1	0.1	0.1
Disallowed region	0	0	0	0	0
B-factors (Å^2)					
IDE	36.7	31.2	33.5	29.9	33.1
Substrate	59.9	41.6	44.0	44.5	54.7
solvent	44.5	40.9	45.2	38.4	41.1

[a] $\boldsymbol{N}_{obs}/\boldsymbol{N}_{unique}$.

[b] $\boldsymbol{R}_{sym} = \sum_{hkl}\sum_{i}|I_i (h\ k\ l)-\langle I (h\ k\ l)\rangle| / \sum_{hkl}\sum_{i} I_i (h\ k\ l)$ for n independent reflections and i observations of a given reflection; $\langle I (h\ k\ l) \rangle$ is the average intensity of the i observations.

[c] The outer resolution shell.

[d] $\boldsymbol{R}_{work} = \sum_{hkl} F_{obs} - F_{calc} / \sum_{hkl} F_{obs}$.

[e] $\boldsymbol{R}_{free}$, calculated the same as for $\mathbf{R}_{work}$ but on the 10% data excluded from the refinement calculation.